ARTICLE

Check for updates

Predictable maternal separation confers adult stress resilience via the medial prefrontal cortex oxytocin signaling pathway in rats

Dong-Dong Shi[1,2], Ying-Dan Zhang[1], Yan-Yan Ren[1], Shi-Yu Peng[1], Ti-Fei Yuan[1] and Zhen Wang[1,2,3]✉

Early-life stress is normally thought of as a major risk for psychiatric disorders, but many researchers have revealed that adversity early in life may enhance stress resilience later in life. Few studies have been performed in rodents to address the possibility that exposure to early-life stress may enhance stress resilience, and the underlying neural mechanisms are far from being understood. Here, we established a "two-hit" stress model in rats by applying two different early-life stress paradigms: predictable and unpredictable maternal separation (MS). Predictable MS during the postnatal period promotes resilience to adult restraint stress, while unpredictable MS increases stress susceptibility. We demonstrate that structural and functional impairments occur in glutamatergic synapses in pyramidal neurons of the medial prefrontal cortex (mPFC) in rats with unpredictable MS but not in rats with predictable MS. Then, we used differentially expressed gene (DEG) analysis of RNA sequencing data from the adult male PFC to identify a hub gene that is responsible for stress resilience. Oxytocin, a peptide hormone, was the highest ranked differentially expressed gene of these altered genes. Predictable MS increases the expression of oxytocin in the mPFC compared to normal raised and unpredictable MS rats. Conditional knockout of the oxytocin receptor in the mPFC was sufficient to generate excitatory synaptic dysfunction and anxiety behavior in rats with predictable MS, whereas restoration of oxytocin receptor expression in the mPFC modified excitatory synaptic function and anxiety behavior in rats subjected to unpredictable MS. These findings were further supported by the demonstration that blocking oxytocinergic projections from the paraventricular nucleus of the hypothalamus (PVN) to the mPFC was sufficient to exacerbate anxiety behavior in rats exposed to predictable MS. Our findings provide direct evidence for the notion that predictable MS promotes stress resilience, while unpredictable MS increases stress susceptibility via mPFC oxytocin signaling in rats.

Molecular Psychiatry (2021) 26:7296–7307; https://doi.org/10.1038/s41380-021-01293-w

INTRODUCTION

Early-life stress increases the risk for psychiatric disorders. A number of epidemiological studies strongly support an association of early-life stress with increased vulnerability to develop psychopathology later in life [1, 2]. However, many examples have shown that adversity early in life may enhance stress resilience in adulthood [3–5]. Stressors throughout early life showed a positive relationship with later-life resilience [6]. Adolescents who had experienced moderate childhood stress showed an attenuated depressive response following proximal stressors [7]. Despite the clinically observed effect of early-life stress effects on resilience, its biological basis remains unknown. Few studies have been performed in rodents about the possibility that exposure to early-life stress may enhance stress resilience in adulthood. Understanding the biological basis of such stress resilience may illuminate causal mechanisms underlying early-life stress and shed light on preventive methods for stress susceptibility.

Maternal separation is one of the most frequently used early-life stress paradigms [1, 8]. Separation from pups renders adult mice more vulnerable to depression-like behavior after adult stress [9], showing that early-life stress increases the risk for depression [10]. However, separation from the pups attenuates the effect of adolescent social isolation on the hypothalamic-pituitary-adrenal (HPA) axis responsiveness in adult rats [11], which indicates that aversive experiences early in life trigger adaptive processes and then render an individual better able to cope with aversive stress later in life. The opposite results may be attributed to the length and period of maternal separation (MS). Various protocols dramatically affect the outcome of behaviors of adult animals exposed to MS [12]. At present, there is no general consensus on what differentiates moderate versus severe forms of MS.

Individuals are continually faced with aversive events as they go through life, and these events can either be predictable or unpredictable. Thus, we adapted two different MS paradigms, such that rats were either raised under the standard set of conditions (standard reared) or subjected to predictable or unpredictable MS. Predictable MS (PMS) rats showed no anxiety-

[1]Shanghai Mental Health Center, Shanghai Jiao Tong University School of Medicine, Shanghai, China. [2]Shanghai Key Laboratory of Psychotic disorders, Shanghai Mental Health Center, Shanghai Jiao Tong University School of Medicine, Shanghai, China. [3]Institute of Psychological and Behavioral Science, Shanghai Jiao Tong University, Shanghai, China. ✉email: wangzhen@smhc.org.cn

Received: 25 January 2021 Revised: 20 August 2021 Accepted: 8 September 2021
Published online: 24 September 2021

and depression-like behavior, while unpredictable MS (UMS) rats showed obvious anxiety- and depression-like behavior in adulthood, indicating that UMS can have long-lasting adverse effects on rat behavior, but PMS does not. To further understand the long-lasting effects of PMS, a second stress, restraint stress, was introduced to rats in adulthood. Amazingly, we show that PMS rats exhibit lower anxiety levels than standard-reared and UMS rats, which means that PMS leads to stress resilience in adulthood. Traditional theories emphasize the stress-reducing role of predictability [13]. To understand the underlying mechanism of PMS and UMS on resilient and vulnerable effects, we revealed that oxytocin (OXT), a neuropeptide hormone with important functions in the control of social and anxiety behaviors, in the medial prefrontal cortex (mPFC) impacts the behaviors of rats. Numerous studies in both humans and rodents broadly illustrate the mPFC as a vital part of the brain that regulates stress resilience [14]. We show that manipulating OXT and its receptor (OXTR) in the mPFC preferentially affects PMS resilience behavior and UMS vulnerability behavior. Collectively, our results indicate that predictable maternal separation reduces stress reactions and improves stress resilience in rats, identifying oxytocin as an important molecular regulator of PMS stress-reducing effects.

MATERIALS AND METHODS

Rats

All procedures involving rats were approved by the Institutional Animal Care and Use Committee at Shanghai Jiao Tong University and in accordance with the National Institutes of Health guidelines. Animals were housed in fully equipped facilities in the laboratory animal center of Shanghai Jiao Tong University. SD rats (Jackson Labs) were used in our experiments. Two SD females were mated with one male per animal facility. The male was removed after one week, and the females were separated into individual cages 1–3 days prior to giving birth. On the day of birth (postnatal day (PND) 0), the pups were weighed and counted, and the cages were cleaned but otherwise undisturbed. Cages were cleaned with minimal disruption to the litter once a week. Offspring were weaned at postnatal PND 21, with males and females weaned separately into cages of 3–4 rats, keeping littermates together. In these experiments, young SD rats at PND 4–90 were used. All testing was performed with male offspring rats. Rats were housed three to four per cage and maintained on a 12/12-h light/dark cycle at 23 °C with water and food available ad libitum. Littermates of the same sex were randomly assigned to different experimental groups.

Early-life stress

The early-life stress paradigm was adapted from established rat paradigms of maternal separation for 2–4 h/day [15]. Postnatal stress was administered for 16 days from PND 4 to 20. We applied a maternal separation protocol in which whole litters were moved to clean cages apart from their mothers for 4 h/day. For predictable maternal separation, pups were separated from 9:00 to 13:00. For unpredictable maternal separation, pups were separated as shown in Table S1. Offspring survival was not affected by postnatal stress. There was no observable difference in coat condition or barbering behavior. No differences in food or water intake were detectable during testing. Rats were weighed at birth, PND 7, PND 21, PND 45, and PND 65. The weights of mice < PND 21 are an average of all pups in a litter.

Adult restraint stress

Experiments utilized an established restraint stress protocol to induce depression/anxiety-like behaviors in rats. Adults (PND 60–77) were placed in a ventilated plastic cylinder for 2 h per day for 7 consecutive days. Rats were subjected to adult stress by placing them in a restraint cylinder fitted closely to body size, drilled with holes to allow free breathing, and then housed in homecare. Restraint time, duration and frequency were the same among groups. Control rats were moved from the holding room to a test room and handled for 2–4 min before returning to the holding room 2 h later. A subthreshold restraint stress paradigm (2 h per day for 3 consecutive days) was utilized with OXT knockdown to test enhanced vulnerability to stress.

Behavioral procedures

All behavioral testing was conducted during the animals' light cycle, videotaped, and analyzed with video tracking software (Ethovision, Noldus, Netherlands). The order of testing was random.

Anhedonia. Sucrose preference, a measure of anhedonia-like behavior in mice, was assessed in a two-bottle choice test. Rats were acclimated to the presence of two bottles of drinking water (180-mL cylindrical tubes) throughout the day and night. After two days of acclimation, the setup was changed to one bottle of water and one bottle of 1% sucrose solution (prepared in drinking water), and the two bottles were weighed. Bottle locations were switched after 1.5 h. The bottles were weighed again after 3 h. The percent sucrose preference was calculated as the amount (g) of sucrose solution consumed divided by the total amount (g) of water and sucrose solution consumed.

Open field test. The open field apparatus is a 60 × 60 × 60-cm Plexiglas arena with clear walls and a blue floor with a 30 × 30-cm central zone. Testing was performed under dimly light conditions without the presence of experimenters. The test rats were introduced into a corner of the open arena. The total distance and velocity moved and the frequency of transfer between the central and surrounding zones and the duration in the central zones were recorded over a 10-min test period. The apparatus was cleaned with 75% alcohol between tests. No rats were excluded from the open field test.

Novel object/location recognition. Object recognition tasks were performed in the open field arena (60 × 60 × 60 cm). Twenty-four hours prior to the acquisition phase, rats were habituated to the testing environment without objects (pretraining). During testing, objects were placed in the corners of the arena, 5 cm from the walls. Each pretraining, acquisition and retrieval trial lasted 5 min. The percentage of time exploring each object and the discrimination index in the retrieval trial were calculated. In addition, the object preference ratio in the acquisition trials was calculated and summarized. For the novel object recognition task, both the pretraining and the testing procedures consisted of trials separated by an intertrial interval of 2 h. No spatial cue was provided during testing. In the acquisition phase, two identical objects were presented. In the retrieval phase, one of the objects was replaced by a novel object. The discrimination index was calculated as 100% × (time with the novel object-time with the known object) / time with both objects. For the novel location task, both the pretraining and the testing procedures consisted of 2 trials separated by an intertrial interval of 2 h. In the acquisition phase, two identical objects were presented. In the retrieval phase, rats were presented with a nondisplaced object and a relocated object. The discrimination index was calculated as 100% × (time with the relocated object − time with the stationary object) / time with both objects.

Social interaction test. Social interaction behavior was assessed with a novel rat. In the first 5 min, the experimental rat was allowed to freely explore an arena (60 × 60 cm) containing a plexiglass and wire mesh enclosure (15 × 15 cm) centered against one wall of the arena. In the second 5 min, the experimental rat was immediately returned to the arena with a novel rat enclosed in the plexiglass wire mesh cage. Time spent in the "interaction zone" (20 × 20 cm) surrounding the plexiglass wire mesh cage was measured by video tracking software (Ethovision, Noldus). A social interaction ratio was calculated as time spent exploring the interaction zone with the target present divided by time spent exploring the arena.

Elevated plus maze. The apparatus consisted of two open arms (60 × 15 cm) and two closed arms (60 × 15 cm) with roofless gray walls (50 cm) connected by a central square platform (15 × 15 cm) and positioned 60 cm above the ground. The test rat was placed in the center zone of the EPM facing an open arm. Rats were allowed to move freely in the maze for 5 min. The distance moved, the time spent in each arm and the number of entries into each arm were automatically analyzed by Noldus software. Animals that fell off the open arms were excluded from analyses. The apparatus was cleaned with 75% alcohol between tests.

Corticosterone assay

Corticosterone concentrations were measured in rat serum. Tail venous blood was collected from an independent cohort of standard-reared and early-life stress rats at PND 56 (before restraint stress), PND 57 (first day

restraint stress) and PND 64 (last day restraint stress). Blood (2.0–2.5 mL) was obtained after behavioral tests via cardiac puncture. At both time points, blood was allowed to clot for 2 h at room temperature, centrifuged at 2000 *g* for 20 min at 4 °C, and serum was removed and stored at −80 °C. Corticosterone was quantified by enzyme-linked immunosorbent assay (parameter corticosterone assay KGE009, R & D systems) according to assay instructions with the following modifications: 50 µL of serum and 50 µL of pretreatment E were used and further diluted to a final dilution factor of 4. All samples were run in duplicate, counterbalanced across plates and were within the standard curve.

Viral vectors

AAV9-shRNA vectors against OXTR (1.34×10^{13} GC/mL) were purchased from Vigene Bioscience (China) with scrambled shRNA (4.61×10^{13} GC/mL) as a negative control. AAV9-OXTR was also provided by Vigene Bioscience (China). The rat OXTR sequence (NM_012871.3) with a C-terminal 3 × FLAG tag was synthesized and inserted into the Pav-CMV-P2A-GFP vector, which separately expresses an OXTR-3 × FLAG fusion protein and green fluorescent protein (GFP) reporter. The titer of AAV-CMV-OXTR-P2A-GFP was 2.20×10^{12} GC/mL, and the titer of AAV-CMV-GFP was 1.36×10^{12} GC/mL. AAV-OXT-DIO-hM4D(Gi)-mCherry (1.23×10^{13} GC/mL) and AAV-CMV-betaglobin-Cre-P2A-GFP (4.61×10^{13} GC/mL) were both purchased from Vigene Biosciences.

Stereotaxic surgery

Rats were anesthetized with isoflurane (R510-22, RWD China, 4–5% induction, 1–2% maintenance) in O_2 by inhalation and positioned in a stereotaxic frame. The skull surface was exposed, and 33-gauge syringe needles (Hamilton) were used to bilaterally infuse AAV virus at a rate of 0.067 µL/min. Brain coordinates of injections were chosen in accordance with the rat brain atlas: mPFC (AP: +3.0 mm; l: ±0.60 mm; DV: −1.72 mm) and PVN (AP: −0.26 mm; l: ±0.20 mm; DV: −7.60 mm). Rats that had been injected with AAVs were allowed 3 weeks to recover and for the viral transgenes to be adequately expressed before undergoing behavioral experiments. The injected volume viruses were 1 µL for the mPFC and 0.5 µL for the PVN. Animals with spatially inaccurate viral injections or significant viral spread outside the targeted region were excluded from analyses. For infusion experiments, double guide cannulae were implanted following bilateral craniotomy and attached to the skull using dental cement. Behavioral tests were performed 2 weeks after surgery. Twenty-five minutes before RS, a treatment consisting of saline, OXT (1 µg/µL, Sigma–Aldrich) or an OXT antagonist (50 µg/µL, Tocris) was infused in a volume of 1 µL through the internal cannula inserted in the guide cannula.

Drugs

At least 3 weeks after injections, we inhibited PVN OXT release by i.p. administration of clozapine N-oxide (CNO, Abcam) dissolved in physiological saline (0.9% NaCl) at a dose of 3 mg/kg in a volume of 1 mL/kg 30 min before the behavioral test. For control experiments, the same volume of saline was injected into the same rats. After the behavioral test, rats received 2 h of restraint stress.

Brain slice preparation

Rats were anesthetized with isoflurane and perfused with 50 mL chilled dissection buffer (25.0 mM $NaHCO_3$, 1.25 mM NaH_2PO_4, 2.5 mM KCl, 0.5 mM $CaCl_2$, 7.0 mM $MgCl_2$, 25.0 mM glucose, 110.0 mM choline chloride, 11.6 mM ascorbic acid and 3.1 mM pyruvic acid, gassed with 95% O_2 and 5% CO_2). Coronal mPFC slices of 300 µm thickness were sectioned in chilled dissection buffer with a VT1000s vibratome (Leica). Slices were incubated in oxygenated artificial cerebrospinal fluid (ACSF), left to recover for 90 min at 37 °C, and transferred to room temperature until the electrophysiological recordings.

Electrophysiological recordings

Slices were continuously perfused with ACSF at ~4 mL/min in the recording chamber. Slices were visualized under a Zeiss microscope station equipped with a camera. Slices equilibrated in the chamber for >10 min before recordings. Recordings were made with borosilicate glass pipettes pulled on a Sutter Instrument P-97 micropipette puller. The resistance ranged between 2 and 5 MΩ following fire polishing to enhance seal quality. For current clamp recordings, the intracellular solution contained (in mM) 130 K gluconate, 5 KCl, 10 HEPES, 2.5 $MgCl_2$, 4 Na_2ATP, 0.4 Na_3GTP, 10 Na phosphocreatine, 0.6 EGTA. For voltage clamp recordings, the intracellular solution contained (in mM) 115 $CsMeCO_3$, 20 CsCl, 10 HEPES, 2.5 $MgCl_2$, 4 Na_2ATP, 0.4 NaGTP, 10 Na phosphocreatine, and 0.6 EGTA. Current clamp recordings were filtered at 2.5 kHz and sampled at 5 kHz. Voltage-clamp recordings were filtered at 2.5 kHz and sampled at 10 kHz. To examine the effect of MS on the excitability of pyramidal neurons in the mPFC, we injected sequential currents from −50 pA to 400 pA in a 50 pA step for 500 ms. The current was injected every 60 s in the current clamp. Electrophysiological recordings were performed under double-blind conditions.

Lucifer yellow labeling by intracellular injection

Rats were perfused with 4% paraformaldehyde (PFA) in PBS, and their brains were removed to perform intracellular injection of the fluorescent dye Lucifer yellow. The brains were postfixed for 24 h in 4% PFA in PBS, and coronal sections were obtained (300 µm). Sections were placed under a differential interference contract (DIC) microscope to find pyramidal neurons in the mPFC, and a continuous current (5–10 nA) was used to inject cells with Lucifer yellow. At least 5 pyramidal cells per rat were injected individually with Lucifer yellow, with the current applied until the distal tips of each dendrite fluoresced brightly (10 min). Images for spine density counting were acquired using a two-photon microscope (OLYMPUS FV1000) with a 20X objective. Spine counting and spine morphology analyses were performed using ImageJ 1.53a software.

Immunohistochemistry and imaging

PND 70 males were terminally anesthetized with isoflurane and 2% chloralhydrate and transcardially perfused with PBS followed by 4% paraformaldehyde (PFA), and brains were postfixed 24 h in 4% PFA at 4 °C. Brains were then dehydrated in 30% sucrose at 4 °C until sinking to the bottom of the 50 mL tube. Coronal sections were made on a freezing vibratome at 30 µm. Sections of selected areas were washed in PBS three times for 10 min, blocked by incubation in PBS plus 4% normal goat serum and 0.1% Triton X-100 for 1 h at room temperature and subsequently incubated with c-fos antibody (1:5000, rabbit, Invitrogen) at 4 °C overnight. Incubated slices were washed three times in PBS for 10 min at RT, incubated for 2 h with a 1:1000 dilution of Alexa Fluor 488 goat anti-rabbit IgG (1:1000, Thermo Fisher Scientific) at RT and subsequently washed three times in PBS for 10 min at RT. The sections were mounted on slides and coverslipped.

All images were obtained using LSM780 confocal microscopes (Zeiss). Digitalized images were analyzed using Fuji (NIMH, Bethesda MD, USA), and Adobe Photoshop CS5 (Adobe, Montain View, CA) was used to increase the contrast of the picture without affecting its real color.

RNAscope

Fluorescence in situ hybridization (FISH) for OXTR mRNA was performed using an RNAscope Fluorescent Multiplex 2.0 assay as per the manufacturer's instructions (Advanced Cell Diagnostics). Briefly, fresh whole rat brains were embedded in OCT medium and quickly frozen in 2-methylbutane chilled to −80 °C. Cryosections of the PFC (cut at a thickness of 10 µm) were then prepared and mounted on SuperFrost Plus slides. Sections were fixed and pretreated according to the RNAscope guide for fresh frozen tissue. After pretreatment, sections were hybridized with FISH probes using a HybEz Hybridization System. After several amplification sets, the sections were counterstained with DAPI and mounted using Prolong Gold. Reactive cells were analyzed bilaterally in the NAc. Confocal images were acquired on an LSM 780 confocal microscope.

RNA isolation, qPCR, library preparation and sequencing

Total RNA was isolated from frozen dissected PFC tissue using QIAzol lysis reagent and purified using a miRNAeasy mini kit (Qiagen). cDNA was obtained from total RNA using a high capacity cDNA Reverse Transcription Kit (Life Technologies). All polymerase chain reaction (PCR) experiments were conducted in duplicate using SYBR Premix Ex Taq (Takara Bio), and fluorescent SYBR Green signals were automatically detected and analyzed with a CFX96 Touch Real-Time PCR Detection System (Bio-Rad) or Applied Biosystems 7500 (Applied Biosystems). The primers for PCR are shown in Table S5. The values were normalized to those of GAPDH mRNA in the same cDNA samples. The levels were then normalized to those of the control groups. Total RNA was prepared using an RNeasy Plus Mini kit (QIAGEN). The resultant RNA (35 ng per array isolated from the mPFC of an

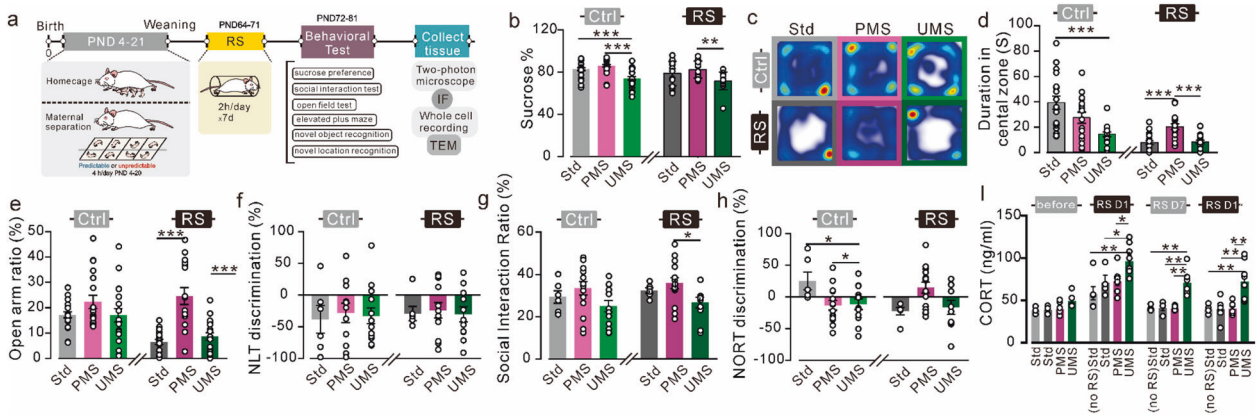

Fig. 1 Maternal separation affects stress susceptibility and resilience in adult rats. a Schematic timeline and behavioral paradigm in rats, maternal separation (MS) was performed from PND 4–20 days, followed by group housing, and subsequent sucrose preference test (SPT) in adult rats, and subsequent restraint stress from PND 64–71, followed by SPT, open field test (OFT), novel location test (NLT), novel object recognition test (NORT) and elevated plus maze teat (EPM). **b** Behavioral effects of maternal separation (MS) and restraint stress (RS) in sucrose preference test. There was a main effect of MS on sucrose preference ($F_{2,90} = 19.10$, $P < 0.0001$). Among control rats, UMS rats showed a decreased preference for sucrose relative to PMS and standard-reared (Std) rats (Bonferroni post-test $P < 0.01$). There was a main effect of RS on sucrose preference ($F_{2,52} = 6.075$, $P = 0.004$). Among RS rats, sucrose preference in UMS rats was significantly lower than PMS rats (Bonferroni post-test $P = 0.003$, from left to right in the figure panel: $n = 28$, 34, 31, 18, 21, and 16 rats). **c** Heatmap of average rat exploration during open field test. **d** Duration in central zone in open field test. UMS rats spent less time in central zone compared to Std rats (Brown–Forsythe and welch ANOVA tests, Dunnett's T3 post-test $P = 0.0006$). There was a main effect of RS on anxiety-like behavior in the center of an open field ($F_{2,48} = 9.297$, $P = 0.0004$). PMS rats spent more time in central zone compared to Std and UMS rats after RS (Bonferroni post-test $P < 0.0001$, from left to right in the figure panel: $n = 18$, 16, 17, 19, 17, and 20 rats). **e** Open arm ratio in elevated plus maze test. After RS, PMS rats spent more time in open arms compared to Std and UMS rats (Brown–Forsythe and welch ANOVA tests, Dunnett's T3 post-test $P = 0.0002$; 0.0008, from left to right in the figure panel: $n = 23$, 18, 19, 20, 16, and 20 rats). **f** No difference was observed in novel location recognition (from left to right in the figure panel: $n = 6$, 11, 13, 6, 12, and 11 rats). **g** There was a main effect of RS on depression-like behavior in social interaction ratio ($F_{2,29} = 3.709$, $P = 0.04$). Among RS rats, social interaction ratio was reduced among UMS vs. PMS rats (post-hoc, $P = 0.03$, from left to right in the figure panel: $n = 6$, 14, 13, 6, 15, and 11 rats). **h** PMS and UMS showed poor novel objective recognition than control rats (one-way ANOVA, $F_{2,29} = 3.912$, $P = 0.031$, post-hoc, $P = 0.033$). But after restraint stress, PMS had an elevated discrimination ratio than other groups (one-way ANOVA, $F_{2,29} = 4.455$, $P = 0.021$, from left to right in the figure panel: $n = 6$, 14, 12, 6, 15, and 10 rats). **i** The concentration of corticosterone in serum of rats at different time points in adult rats. The baseline of corticosterone in serum was at the same level. The concentration of corticosterone in UMS rats was significantly higher than control, restraint stress and PMS ($P < 0.05$) groups on PND 57 (the first day of restraint stress). And on the 7th day and after restraint stress, corticosterone in UMS was still kept in high level compared with other groups ($P \leq 0.008$, $n = 4$–7). $^*P < 0.05$, $^{**}P < 0.01$, $^{***}P < 0.001$. Bar graphs show the mean ± s.e.m.

individual mouse) was converted to cDNA using a Low Input Quick Amp Labeling Kit (Agilent Technologies). The cDNA samples were used to synthesize Cy3-labeled cRNA using a Low Input Quick Amp Labeling Kit (Agilent Technologies). The resultant Cy3-labeled cRNA was fragmented and hybridized with a SurePrint G3 Mouse GE 8 3 60 K Microarray (Agilent Technologies).

Statistics and reproducibility

All data were analyzed for statistical significance using GraphPad Prism software. G*Power 3.1.9.7 software was applied to calculate the power of the sample size. For multiple groups or multiple measures, we used one-way or two-way analysis of variance (ANOVA). For multiple groups or multiple measures, we first used the normality and lognormality tests to assess the normality of the distribution. A $p > 0.05$ means that the distribution is normal. A $p < 0.05$ means that data do not follow the normal distribution; in this case, nonparametric tests should be used. Normally distributed data will be subjected to a homogeneity of variance test. The Brown-Forsythe test and Bartlett's test were used to test the homogeneity of variance. If the significance level was >0.05, then homogeneity was met; if it was $p < 0.05$, then it was violated, and Brown-Forsythe and Welch ANOVA tests were used. Tukey's multiple comparisons tests were used for one-way ANOVAs with multiple comparisons across groups. Bonferroni's multiple comparison tests were used for between-subject comparisons after two-way ANOVA, and Fisher's single comparison tests were used for a within-subject comparison. All behavioral tests were repeated in a minimum of three cohorts with similar replication of results. Data for imaging and electrophysiology experiments were pooled from at least three individual animals. Littermates were randomly assigned to experimental groups, and animals were tested in a random order. Data were analyzed by an investigator blinded to the experimental conditions, and the experimenter was not blinded during data collection.

RESULTS

Predictable maternal separation improves adult stress resilience, while unpredictable maternal separation confers susceptibility to anxiety from restraint stress

To test the effects of different levels of early-life stress on adult stress reactions, we adapted a maternal separation protocol of early-life stress in rats and tested two different exposure paradigms, predictable and unpredictable. Rats were either standard reared or subjected to predictable or unpredictable early-life stress (Fig. 1a). Early-life stress in both paradigms did not affect offspring survival, although both predictable and unpredictable stress initially slowed weight gain measured at weaning, followed by increased weight gain by adulthood (Supplementary Fig. 1a). In male rats, predictable maternal separation (PMS) did not produce detectable behavioral effects, while UMS rendered adult rats more susceptible to depression-like behavior (anhedonia in sucrose preference test) (Fig. 1b) and anxiety-like behavior (open field test) before adult stress (Fig. 1c–e). We assessed the impact of early-life stress on adult male stress resilience and susceptibility using the restraint stress paradigm from postnatal day (PND) 72–81. Restraint stress decreased the duration in the central zone in the open field test and the open arm ratio in the elevated plus maze in standard-reared rats and unpredictable MS rats (Fig. 1c, e). In PMS group rats, anxiety level was significantly lower than that of UMS and standard-reared rats after adult restraint stress (Fig. 1d, e), suggesting that PMS showed greater resiliency to restraint stress anxiety than standard-reared (Std) or UMS rats. Early-life stress had no effects on novel location and social interaction behavior in PMS and UMS rats before RS.

However, in the novel objection recognition test, both PMS and UMS rats spent less time exploring the novel objection before RS. After restraint stress, the social interaction rate was significantly lower than that of PMS rats (Fig. 1f–h). Neither early-life stress MS nor adult restraint stress had effects on locomotor behavior.

We detected the corticosterone (CORT) concentration in serum on PND 21 and PND 64–71. There was no difference among these three groups in corticosterone levels under baseline conditions. On restraint stress day one, corticosterone levels increased in rats subjected to restraint stress. After 7 days of habituation, the corticosterone levels returned to baseline in standard-reared and PMS rats, while they remained high in UMS rats (Fig. 1i).

UMS injured the neuronal morphology of pyramidal neurons in the mPFC, while PMS did not

Many studies have explored the central pathways mediating the stress response by mapping neuronal activation using c-fos mapping. To identify target brain subregions through which mild early-life stress mediates its anti-anxiety effects, we detected c-fos mapping followed by open field test in 90 min. C-fos-labeled neurons were quantified every 120 μm throughout the rostral-caudal extent of the brain based on anatomic registration according to an existing brain atlas (Supplementary Fig. 2a). In total, we identified 17 brain regions that consistently displayed c-fos labeling (Supplementary Fig. 2a). In the claustrum, RSD, Tu and mPFC regions, we found that c-fos expression was significantly lower in UMS rats than in Std and PMS rats. As expected, we identified the mPFC as the targeted brain region that mediated anxiety-like behavior. The mPFC c-fos expression in PMS rats was significantly higher than that in standard-reared and UMS rats (Supplementary Fig. 2b, c). This finding indicates that the mPFC might play an essential role in early-life stress effects on adult stress reactions.

Early-life stress has a harmful effect on structural and functional changes in neurons. First, we examined the dendritic spines of mPFC pyramidal neurons in standard-reared rats and MS rats (Fig. 2a). UMS rats exhibited lower spine density (Fig. 2f). To examine how maternal separation relates to dendritic spines, we classified dendritic spines into three categories based on the maximal diameter of the spine head and the length of spines (thin spines maximal diameter < 0.60 μm and length > 0.9 μm, mush-room spines maximal diameter < 0.60 μm and length < 0.9 μm, and others) [16, 17]. UMS rats displayed fewer thin spines and mushroom spines than Std and PMS rats (Fig. 2g). Second, electron microscopy results indicated that the mean length and thickness of postsynaptic densities were significantly lower in UMS rats than in standard-reared and PMS rats (Fig. 2b–d). Together, these results indicate that UMS leads to structural defects in the dendrites and spines of mPFC pyramidal neurons. To further confirm the resilient effect of PMS, we detected synaptic structures after restraint stress. Our results showed that the mean length and thickness of postsynaptic densities were significantly lower in Std and UMS rats than in PMS rats after restraint stress (Supplementary Fig. 3a–c). These results suggested that PMS promote stress resilience to restraint stress.

UMS impairs the synaptic function of pyramidal neurons in the mPFC, while PMS does not

To determine whether MS alters mPFC excitability, the frequency of action potentials in response to depolarizing current steps was measured from mPFC pyramidal neurons. The number of action potentials elicited (induced spikes) over an interval of 500 ms was measured, as the current was varied in steps of 50 pA from −50 pA to 400 pA (Supplementary Fig. 4). Pyramidal neurons were characterized as cells that displayed spike-frequency adaptation and broad action potentials and lacked spontaneous discharge at resting membrane potential. Depolarizing currents evoked higher firing in the std and PMS rats than in the UMS rats (Supplementary Fig. 4b). Similarly, less current was required to drive the cell to fire spikes at a given frequency (Supplementary Fig. 4b).

To examine the functional consequences of MS on synaptic transmission in the mPFC, we performed whole-cell patch-clamp recording of pyramidal neurons. We first examined spontaneous excitatory postsynaptic and inhibitory postsynaptic currents (sEPSCs and sIPSCs, respectively). sEPSCs and sIPSCs were recorded in the same cells by alternate clamping at the reversal potential of GABA receptor-mediated (−70 mV) and glutamate receptor-mediated (0 mV) currents, respectively (Supplementary Fig. 4). The sEPSC amplitude was decreased in UMS rats compared to standard-reared and PMS rats, while the sIPSC amplitude was comparable among the three groups. Consequently, the sEPSC/sIPSC ratio of amplitude was decreased significantly in UMS rats. For sEPSC frequency, there was no difference among groups. For sIPSC frequency, UMS was significantly lower than std and PMS rat. However, the EPSC/IPSC ratio of frequency was comparable among std, PMS and UMS rats (Supplementary Fig. 4d–j).

Furthermore, we found that the peak amplitude of α-amino-3-hydroxy-5-methylisoxazole-4-propionic acid receptor (AMPAR)-mediated miniature excitatory postsynaptic currents (mEPSCs) was significantly lower in UMS rats than in std and PMS rats (Fig. 2i–k). To examine whether a dysfunction in presynaptic release contributes to the observed synaptic defects, we performed paired-pulse ratio (PPR) analysis to detect any changes in the probability of presynaptic release. No difference was detected in the PPR among these three groups (Fig. 2l–m), suggesting a comparable postsynaptic response among Std, PMS and UMS rats. The peak amplitude and frequency of mEPSCs in PMS rats were significantly higher than those in std and UMS rats after restraint stress, which suggested the resilient effects of PMS (Supplementary Fig. 3d–f).

Predictable maternal separation upregulates the oxytocin pathway in the mPFC, but unpredictable maternal separation does not

Given the observed difference in PMS- and UMS-induced changes in neuronal structure and neurotransmission, the neuronal molecular mechanisms among these groups were assessed. To capture transcriptome-wide alterations in the adult male mPFC after maternal separation, we used RNA sequencing (RNA-seq) analysis. PMS altered the expression of 114 genes ($P < 0.05$, |fold change| > 2), and UMS altered the expression of 289 genes ($P < 0.05$, |fold change| > 2) compared with standard-reared controls. Differentially expressed genes (DEGs) were enriched for several relevant gene ontology terms (Fig. 3a, Supplementary Fig. 5). GO biological process analysis indicated that PMS exhibited significant differences in genes involved in the pathways of response to glucocorticoids, nucleoside metabolic process and regulation of appetite, which have been associated with anxiety and neural plasticity, compared to std. UMS exhibited significant differences in genes involved in the pathways of developmental process, regulation of ion transmembrane transport, ion transport and response to axon injury compared to std. The top GO terms between PMS and UMS were cellular response to interferon-β, parturition and defense response. Although only 16 genes were altered at criteria between predictable and unpredictable MS, the heatmap of DEG lists revealed that genes were altered in the opposite direction (Fig. 3b). DEG analysis identified oxytocin, a peptide hormone that has been shown to contribute to many aspects of social behavior, as the strongest key driver gene of these altered genes (Fig. 3c). Stressful and anxiogenic stimuli result in the release of OXT, which acts as a powerful modulator of anxiety-related behavior. OXT mRNA was upregulated by PMS compared to standard-reared rats. OXT mRNA in the PFC of PMS rats was significantly higher than that of UMS rats (Fig. 3d). The OXT mRNA expression alteration in the PFC was also confirmed by RT-PCR (Fig. 3e). In addition, we detected the oxytocin mRNA level and oxytocin concentration in the PFC after restraint stress. The

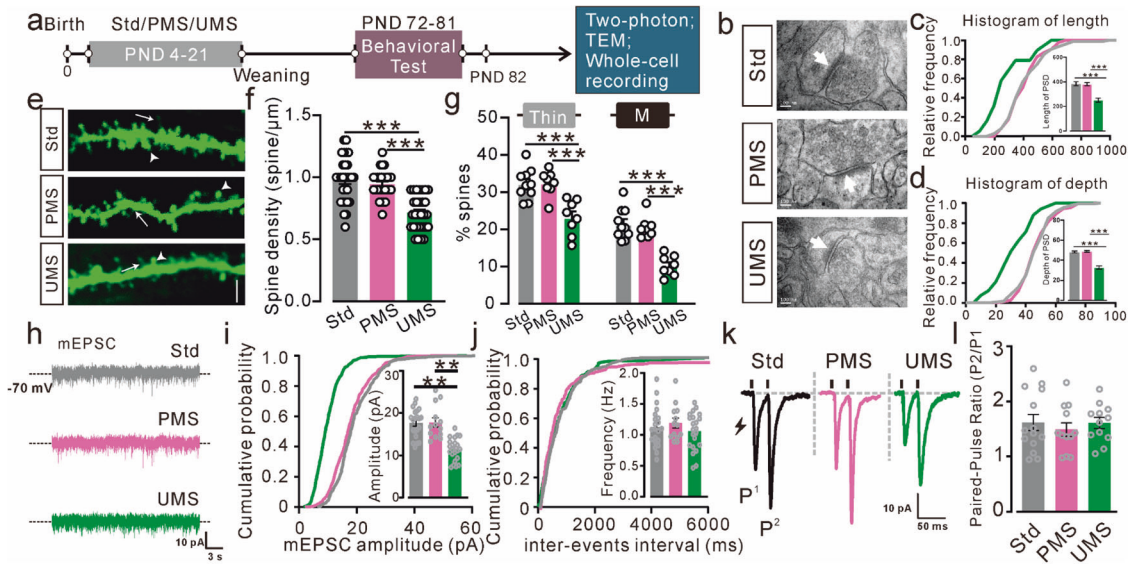

Fig. 2 Morphological changes in the mPFC and excitatory synaptic dysfunction in the mPFC pyramidal neurons of control and MS rats. a Schematic timeline and recording paradigm in rats. **b** Representative electron micrographs showing the synaptic structure and postsynaptic densities on neurons (arrowheads). Scale bar, 100 nm. **c** The lengths of postsynaptic densities were shorter in UMS rats than in control and PMS rats (one-way ANOVA, $F_{2,236} = 25.52$, $P < 0.0001$, CTRL: $n = 76$ synapses from three rats; PMS: $n = 87$ synapses from three rats; $n = 76$ synapses from three rats). **d** The depths of postsynaptic densities were shallower in UMS rats than in control and PMS rats (one-way ANOVA, $F_{2,367} = 54.67$, $P < 0.0001$), CTRL: $n = 163$ synapses from three rats; PMS: $n = 213$ synapses from three rats; $n = 102$ synapses from three rats. **e** Representative confocal stacks and three-dimensional reconstruction images of the apical dendrites of mPFC pyramidal neurons obtained from standard-reared, PMS and UMS rats. Scale bar, 2.5 μm. **f**–**g** spine density and spine morphology were analyzed on the apical dendrites of mPFC pyramidal neurons obtained from control, PMS and UMS rats. Spine density in UMS rats was less than Std ($P < 0.0001$) and PMS ($P < 0.0001$) rats significantly (one-way ANOVA, $F_{2,\ 84} = 27.99$, $P < 0.0001$, $n = 29$ dendrites from three rats). UMS rats displayed less thin spines (two-way ANOVA, Bonferroni post-test $P < 0.0001$) and mushroom spines than Std and PMS rats (two-way ANOVA, Bonferroni post-test $P < 0.0001$). **h** Representative mEPSC of control (black), PMS (red) and UMS (green). Scale bar, 10 pA and 3 s. **i**, **j** There was an effect of MS on mEPSC amplitude (one-way ANOVA, $F_{2,53} = 24.93$, $P < 0.0001$), UMS significantly decreased amplitude compared to control and PMS (post hoc $P < 0.0001$). MS had no effect on mEPSC frequency (one-way ANOVA, $F_{2,53} = 0.811$, $P = 0.450$). **k** Representative PPR of control (black), PMS (red) and UMS (green). Scale bar, 10 pA and 50 ms. **l** There was no effect of MS on PPR. *$P < 0.05$, **$P < 0.01$, ***$P < 0.001$. Bar graphs show the mean ± s.e.m. *$P < 0.05$, **$P < 0.01$, ***$P < 0.001$. Bar graphs show the mean ± s.e.m.

results showed that the oxytocin mRNA level was significantly higher in the PFC of PMS rats than in that of Std and UMS rats (Fig. 3d, e, right). OXT concentration alterations in the mPFC and serum were also evaluated by ELISA. The results showed that in the mPFC, the concentration of oxytocin was higher in PMS compared to UMS both before and after restraint stress (Fig. 3f). In addition, we found that the oxytocin level in UMS serum was lower than that in PMS rats from PND 11 until adulthood (Fig. 3g). We also detected the expression of oxytocin receptors (OXTRs) in the mPFC after restraint stress. Our results showed that the expression of both OXTR mRNA and OXTR protein in PMS rats was significantly higher than that in Std and UMS rats (Supplementary Fig. 5g, h). Together, these results indicate that PMS- and UMS-induced morphological and functional alterations in the mPFC are coupled with changes in the oxytocin-related signaling pathway.

Pharmacological inhibition of oxytocin receptors (OXTR) in the mPFC improves stress susceptibility in PMS rats, and enhancement of OXT improves stress resilience in UMS rats

Since PMS rats exhibited higher OXT levels in the mPFC, we sought to test whether inhibition of OXTR in the mPFC could induce anxiety-like behavior in PMS rats (Fig. 3h, i). L-368,899 hydrochloride, an oxytocin receptor antagonist (OXTRA), was microinjected into the mPFC of PMS rats. The duration in the central zone and open arm ratio in the two groups were in the same line (~45 s in the central zone and 10% open arm ratio) in PMS rats without restraint stress. However, after restraint stress, the PMS rats injected with saline still spent approximately 45 s in the central zones in the open field test and 15% of the time in the open arm in the elevated plus maze, indicating that PMS rats showed robust stress resilience after adult restraint stress (Fig. 3j, k). PMS rats injected with OXTRA spent significantly less time in the central zone and open arms, which demonstrated that the suppression of OXTR ability in the mPFC can induce anxiety-like behavior in PMS rats after restraint stress (Fig. 3j, k). However, whether restraint stress was elicited or not, there was no difference in sucrose preference between oxtra- and saline-treated rats, showing that suppression of OXTR in the mPFC has no effect on depression-like behavior (Fig. 3l).

Given that the profound defect in the oxytocin signaling pathway is the major cause of hypoactivity of mPFC pyramidal cells in UMS, we sought to test whether correcting the reduction in oxytocin in the mPFC could potentially reduce anxiety-like behavior in UMS rats (Fig. 3m). We found that the application of oxytocin had no effects on duration in the central zone or open arm ratio in adult rats without restraint stress (Fig. 3n, o), which means that oxytocin microinjection did not ameliorate the anxiety level induced by unpredictable maternal separation. However, both the time spent in the central zone and the open arm ratio in rats injected with oxytocin were upregulated compared to rats injected with saline, showing that oxytocin in the mPFC can improve stress resilience to adult restraint stress. The sucrose preference level remained at ~60% in UMS rats even after the application of OXT, which indicates that elevated oxytocin in the mPFC was not sufficient to improve anhedonic behavior (Fig. 3p).

To further examine the oxytocin effects in maternal separation rats, we injected OXT/OXTRA by intraperitoneal injection (Supplementary Fig. 6a). Standard-reared rats injected with oxytocin exhibited stress resilience, while rats injected with saline and OXTRA showed obvious anxiety-like behavior (Supplementary

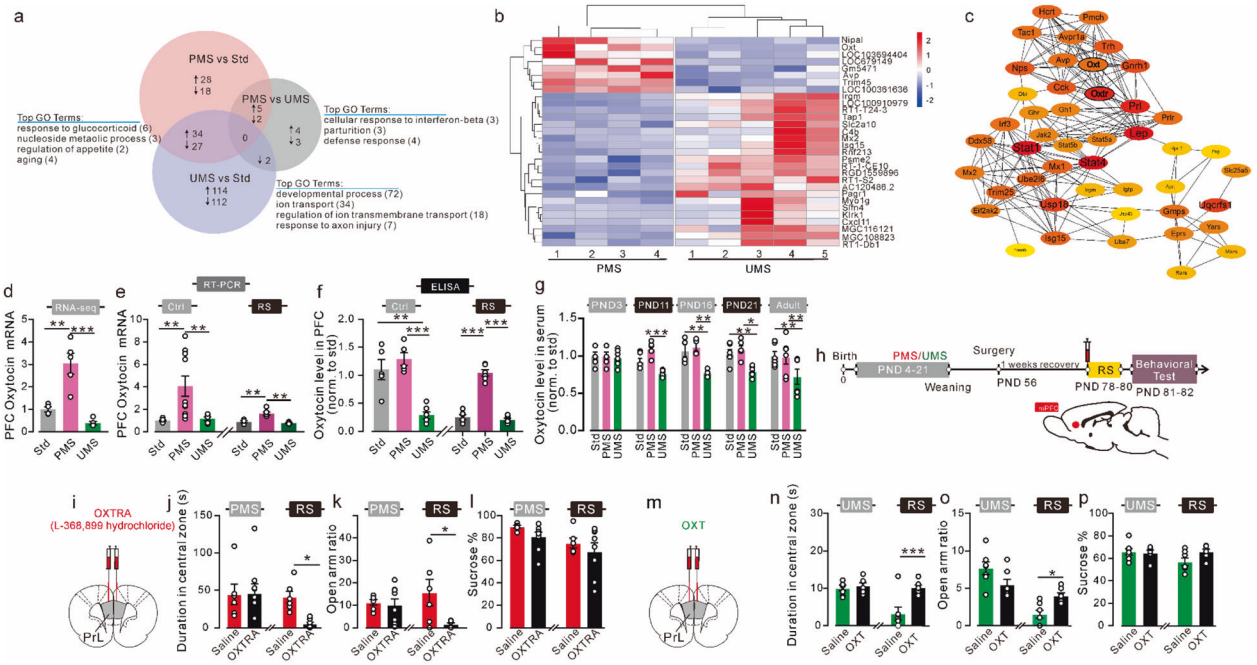

Fig. 3 Analysis of RNA-seq and oxytocin as a differential gene. a Differentially expressed genes (DEGs; $p < 0.05$) and the top associated gene ontology (GO) terms among each indicated comparison. **b** Differentially expressed genes showed in heatmap. Each row corresponds to a single gene. **c** Representation of the different maternal separation-regulated signaling network enrichment analysis including all modules and contributing genes in mPFC region. **d** Oxytocin expression fold change in RNA-seq analysis. **e** Results of RT-PCR showed that the oxytocin expression in mPFC in PMS was higher than standard-reared and UMS rats both before and after RS. **f** Results of ELISA indicated that oxytocin in PFC in PMS and standard-reared rats was higher than UMS rats before RS. After RS, oxytocin level in PMS was significantly higher than Std and UMS rats. **g** The level of oxytocin in serum of rats at different time points in male rats. The baseline (PND 3, before MS) of oxytocin in serum was at the same level. The level of oxytocin in UMS rats was significantly lower than standard-reared and PMS ($P < 0.05$) groups on PND 11 (MS started from PND 4). And from PND 16, oxytocin level in UMS serum was significantly lower compared to other groups ($P \le 0.012$, $n =$ 4–6). **h** Timing of postnatal stress and experimental paradigm of oxytocin antagonist (OXTRA, L-368,899 hydrochloride) via stereotaxic microinjection. **i** illustration of OXTRA and OXT injection into the mPFC. **j** Duration in central zone in open field test (two-way ANOVA, interaction $F_{1,25} = 3.112$, $P = 0.090$, effect of restraint stress $F_{1,25} = 4.432$, $P = 0.046$, effect of OXTRA $F_{1,25} = 2.633$, $P = 0.117$). **k** Open arm ration in elevated plus maze (two-way ANOVA, interaction $F_{1,25} = 4.662$, $P = 0.041$, effect of restraint stress $F_{1,25} = 0.521$, $P = 0.477$, effect of OXTRA $F_{1,25} = 6.298$, $P = 0.019$). After RS, rats injected with OXTRA spent less time in open arm compared to rats injected with saline (Bonferroni post-test, $P = 0.019$). **l** Microinjection OXTRA into mPFC has no effect on sucrose preference in PMS rats (two-way ANOVA, interaction $F_{1,25} = 0.013$, $P = 0.910$). **m** Duration in central zone in open field test (two-way ANOVA, interaction $F_{1,24} = 9.398$, $P = 0.005$, effect of restraint stress $F_{1,24} =$ 12.28, $P = 0.002$, effect of OXT $F_{1,24} = 13.39$, $P = 0.001$). Restraint stress decreased duration in central zone significantly in UMS rats injected with saline (Bonferroni post-test, $P = 0.0006$), while RS has no effect on duration in UMS rats injected with OXT (Bonferroni post-test, $P > 0.999$). After restraint stress, UMS rats injected with OXT spent more time in central zone compared to rats injected with saline (Bonferroni post-test, $P = 0.0005$). **n** Open arm ratio in elevated plus maze (two-way ANOVA, interaction $F_{1,24} = 13.31$, $P = 0.001$, effect of restraint stress $F_{1,24} = 35.91$, $P < 0.0001$, effect of OXT $F_{1,24} = 0.047$, $P = 0.829$). Restraint stress decreased open arm ratio significantly in UMS rats injected with saline (Bonferroni post-test, $P < 0.0001$), while RS didn't reduce the duration in open arms in UMS rats injected with OXT (Bonferroni post-test, $P =$ 0.662). **o** Microinjection OXT into mPFC has no effect on sucrose preference in UMS rats (two-way ANOVA, interaction $F_{1,24} = 3.339$, $P = 0.080$). $^*P < 0.05$, $^{**}P < 0.01$, $^{***}P < 0.001$. Bar graphs show the mean ± s.e.m.

Fig. 6b, c). Unfortunately, no differences were found between PMS rats and UMS rats (Supplementary Fig. 6d–g). These results corroborate the anxiolytic effects of oxytocin in the mPFC. Based on these findings, reducing the oxytocin signaling pathway in the mPFC shifted PMS rats toward a vulnerable phenotype and shifted UMS rats toward a resilient phenotype.

OXTR knockdown in the mPFC promotes stress vulnerability in PMS rats

To test the functions of OXT signaling in stress resilience more accurately, we investigated whether suppressed OXTR in the mPFC was necessary and/or sufficient to promote the behavior associated with resilience (Fig. 4a). We used viral tools to knock down OXTR in the mPFC. Bilateral injection of AAV-oxtr shRNA in the mPFC knocked down OXTR, reducing the expression of OXTR by ~60% (Fig. 4b, c). The concentration of oxytocin in the mPFC in PMS rats injected with AAV-oxtr shRNA was significantly lower than that in AAV-scramble rats (Fig. 4d). Knockdown of OXTR had no effects on anxiety and depression levels in either PMS or standard-reared rats without restraint stress (Fig. 4e, f, Supplementary Fig. 7c, d). AAV-oxtr shRNA rats displayed anxiety-like behavior in the open field (decreased duration in central zones, Fig. 4e) and elevated plus maze (decreased open arm ratio, Fig. 4f) tests. AAV-scramble rats experiencing PMS still showed robust stress resilience to restraint stress (Fig. 4e, f), indicating that OXTR knockdown in the mPFC of PMS rats promoted a more vulnerable phenotype than control AAV-scramble rats. In the standard-reared rats, both AAV-oxtr shRNA and AAV-scramble groups indicated anxiety-like behavior after restraint stress; however, the anxiety level in AAV-oxtr shRNA rats was more severe than that in AAV-scramble rats (Supplementary Fig. 7b, c). However, OXTR knockdown in neither PMS nor standard-reared rats had any effects on sucrose preference (Fig. 4g, Supplementary Fig. 7e), which might be because 3 days of restraint stress cannot induce depression-like behavior. To further explain the effects of OXTR knockdown in the mPFC, we detected behavioral performance two weeks later. The anxiety level was still higher in AAV-oxtr shRNA rats than in AAV-scramble rats (Fig. 4e, f), and the depression level was still the same between the two groups (Fig. 4g).

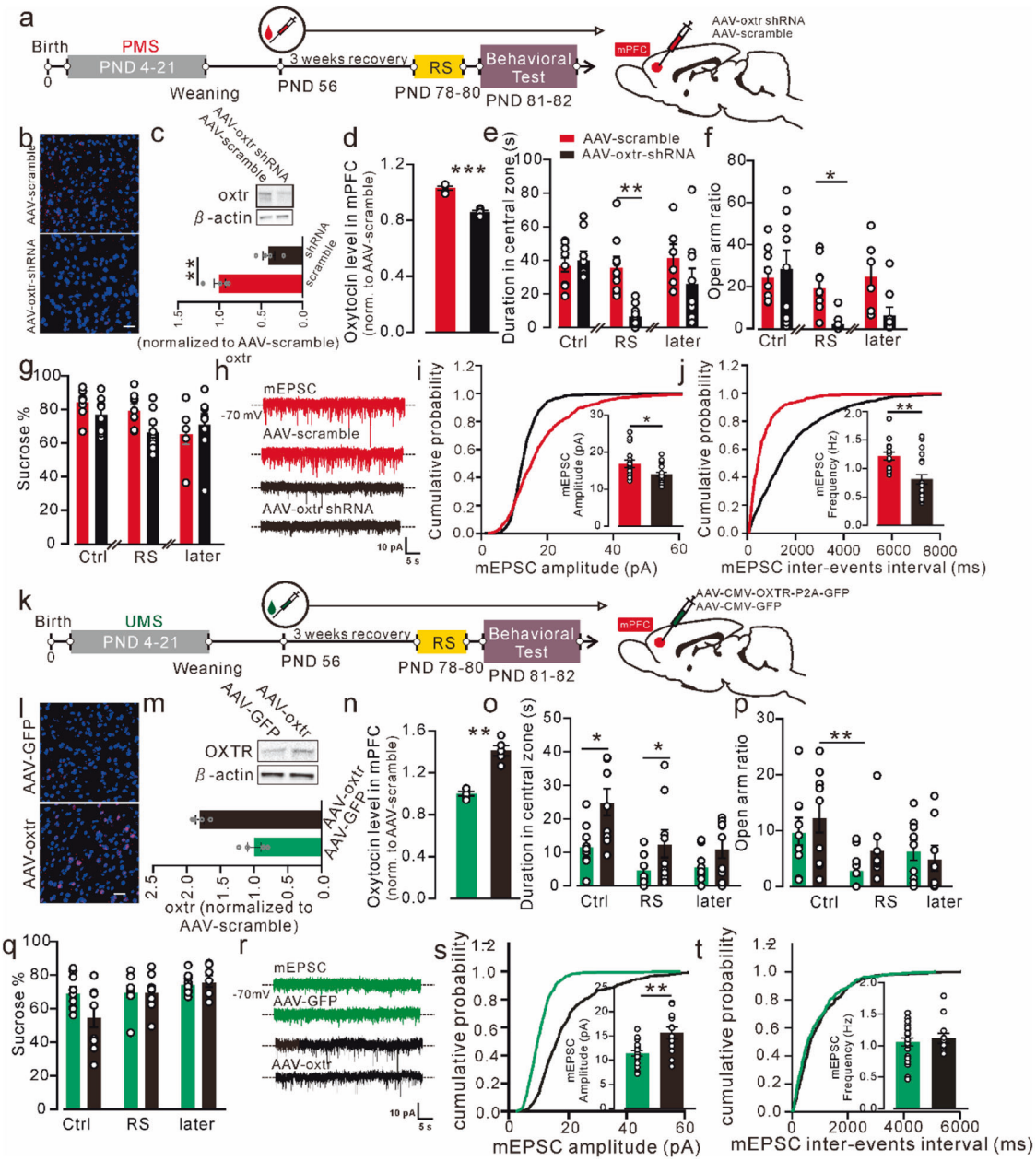

OXTR knockdown decreased mPFC pyramidal cell excitability compared to that in AAV-scramble rats (Supplementary Fig. 8a, b). In addition, OXTR knockdown decreased the sEPSC frequency compared to scramble rats but did not affect the sIPSC frequency or peak amplitude (Supplementary Fig. 8f–k). A decreased sEPSC/sIPSC amplitude ratio was shown in OXTR knockdown rats (Supplementary Fig. 8i, j). OXTR knockdown resulted in a reduction in mEPSC frequency and peak amplitude compared to those of AAV-scramble rats, suggesting that OXTR knockdown altered synaptic transmission function (Fig. 4h–j). These results indicate that reduced OXTR expression in the mPFC shifted PMS rats toward a vulnerable phenotype.

OXTR overexpression in the mPFC promotes stress resilience in UMS rats

To determine whether the overexpression of OXTR in the mPFC promoted stress resilience in UMS rats, we bilaterally administered either AAV-CMV-GFP (control virus, AAV-GFP) or AAV-CMV-OXTR-P2A-GFP (AAV-OXTR), which nonspecifically overexpressed GFP or overexpressed OXTR and GFP, respectively (Fig. 4k). AAV-OXTR increased the expression of OXTR by 50% (Fig. 4l, m). Interestingly, we found that OXTR overexpression in the mPFC ameliorated anxiety-like behavior in the open field test (increased duration in central zones, Fig. 4o) before restraint stress, indicating that OXTR overexpression can rescue UMS-induced anxiety-like behavior. Restraint stress decreased the duration in the central zone and the open arm ratio in both AAV-oxtr UMS rats and AAV-GFP UMS rats. Importantly, in UMS rats, OXTR overexpression rats spent more time in central zones in the open field test than AAV-GFP rats (Fig. 4o, p), showing that OXTR overexpression promoted UMS stress resilience compared to the AAV-GFP control. OXTR overexpression in standard-reared rats improved stress resilience (increased duration in the central zone and increased open arm ratio) compared to AAV-GFP control rats (Supplementary Fig. 9h, i). The behavioral phenotype remained constant two weeks after restraint stress. However, overexpression of OXTR in the mPFC had

Fig. 4 Oxtr knock-down promotes RS induced anxiety-like behavior in PMS rats, and Oxtr overexpression attenuate RS induced anxiety-like behavior in UMS rats. **a** Timing of postnatal stress, AAV manipulation, adult restraint stress and behavior testing and illustration of AAV-U6-OXTR-CMV-GFP injection into the mPFC, representative image of viral targeting of mPFC in adult male rat. **b** Representative image of OXTR mRNA expression in mPFC using RNA Scope. Scale bar, 20 μm. **c** Representative image of OXTR expression in mPFC using western blotting. The OXTR expression in mPFC in AAV-OXTR shRNA rats was decreased significantly compared to AAV-scramble rats (two tailed unpaired *t* test, $P = 0.009$, $n = 4$). **d** Oxytocin concentration in mPFC was decreased significantly in PMS rats injected with AAV-oxtr shRNA compared to rats with AAV-scramble (two tailed unpaired *t* test, $P < 0.001$, $n = 5$). **e** Duration in central zone in open field test (two-way ANOVA, interaction $F_{2,45} = 8.213$, $P = 0.020$; effect of RS $F_{2,45} = 5.066$, $P = 0.010$, effect of AAV $F_{1,45} = 8.213$, $P = 0.006$). Rats injected with AAV-OXTR shRNA stayed less time in central zone compared to rats injected with AAV-scramble (post hoc, $P = 0.010$). **f** Open arm ratio in elevated plus maze test (two-way ANOVA, interaction $F_{2,45} = 3.193$, $P = 0.051$; effect of RS $F_{2,45} = 5.199$, $P = 0.010$, effect of AAV $F_{1,45} = 6.242$, $P = 0.016$). After RS, rats injected with AAV-oxtr shRNA spent less time in open arm compared to before RS (post hoc, $P = 0.041$). **g** There was no difference in sucrose preference test (two-way ANOVA, interaction $F_{2,45} = 2.305$, $P = 0.111$); effect of RS $F_{2,45} = 4.253$, $P = 0.020$, effect of AAV $F_{1,45} = 1.906$, $P = 0.174$. **h** Representative mEPSC of PMS rats injected AAV-scramble (red) and AAV-oxtr shRNA (light red). Scale bar, 20 pA and 200 ms. **i**, **j** Both mEPSC amplitude and frequency in AAV-scramble rats lower than that in AAV-oxtr shRNA rats (two tailed unpaired *t* test, $P \leq 0.014$). $^{*}P < 0.05$, $^{**}P < 0.01$, $^{***}P < 0.001$. Bar graphs show the mean ± s.e.m. **k** Timing of postnatal stress, AAV manipulation, adult restraint stress and behavior testing, illustration of AAV-U6-OXTR-CMV-GFP injection into the mPFC. **l** Representative image of OXTR mRNA expression in mPFC using RNA Scope. Scale bar, 20 μm. **m** Representative image of OXTR expression in mPFC using western blotting. The OXTR expression in mPFC in AAV-OXTR rats was increased significantly compared to AAV-GFP rats (two tailed unpaired *t* test, $P = 0.008$, $n = 4$). **n** Oxytocin concentration in mPFC was upregulated significantly in UMS rats microinjected with AAV-OXTR compared to rats with AAV-GFP (two tailed unpaired *t* test, $P < 0.001$, $n = 5$). **o** Duration in central zone in open field test (two-way ANOVA, interaction $F_{2,48} = 0.962$, $P = 0.389$; effect of RS $F_{2,48} = 7.567$, $P = 0.001$, effect of AAV $F_{1,48} = 13.41$, $P = 0.0006$). Rats injected with AAV-OXTR stayed more time in central zone compared to rats injected with AAV-GFP (Bonferroni post-test, $P = 0.037$). **p** Open arm ratio in elevated plus maze test (two-way ANOVA, interaction $F_{2,46} = 0.749$, $P = 0.479$; effect of RS $F_{2,46} = 5.092$, $P = 0.010$, effect of AAV $F_{1,46} = 0.827$, $P = 0.368$). **q** There was no difference in sucrose preference test (two-way ANOVA, interaction $F_{2,46} = 2.545$, $P = 0.090$; effect of RS $F_{2,46} = 5.674$, $P = 0.006$, effect of AAV $F_{1,46} = 1.906$, $P = 0.171$). Scale bar, 20 pA and 200 ms. **s** Representative mEPSC of UMS rats injected AAV-GFP (green) and AAV-OXTR (dark green). **r**–**t** mEPSC amplitude in AAV-OXTR rats higher than that in AAV-OXTR rats (two tailed unpaired *t* test, $P = 0.001$). $^{*}P < 0.05$, $^{**}P < 0.01$, $^{***}P < 0.001$. Bar graphs show the mean ± s.e.m.

no effects on sucrose preference in UMS and standard-reared rats (Fig. 4q, Supplementary Fig. 9j). Sucrose preference was always maintained at 70% before and after restraint stress in UMS rats, which means that OXTR overexpression cannot rescue UMS-induced depression-like behavior. However, in standard-reared rats, the sucrose preference remained at 80%, perhaps because restraint stress could not induce depression-like behavior.

OXTR overexpression improved the cell excitability of pyramidal cells in the mPFC in UMS rats (Supplementary Fig. 9a, b). Both sEPSC peak amplitude and sIPSC peak amplitude were increased in OXTR-overexpressing rats compared to AAV-GFP rats, but the frequency did not change (Supplementary Fig. 9c–j). Basal synaptic transmission measurements indicated that in the AAV-oxtr mPFC pyramidal cells, there was a partial rescue of mEPSC peak amplitude but no effect on mEPSC frequency (Fig. 4r–t). Together, these experiments provided strong evidence that the oxytocin signaling pathway in the mPFC is both necessary and sufficient to promote adult anxiolysis in response to restraint stress. The sufficient oxytocin concentration in the mPFC of PMS rats accounts for its resilience to adult restraint stress. The deficit of oxytocin in the mPFC of UMS rats accounts for its susceptibility to adult restraint stress.

PVN oxytocinergic neuron projections to the mPFC are essential for anti-anxiety in PMS rats

In rodents, neurons in the PVN are the main source of OXT projections to the brain. To further confirm that the mPFC oxytocin signaling pathway is implicated in rat stress anti-anxiety behavior, we selectively prevented PVN-mPFC OXT projections (Fig. 5a). We injected retrogradely AAV-CMV-betaglobin-cre-P2A-GFP into the mPFC and injected the PVN with an AAV carrying a double-floxed inverted open reading frame (ORF) (DIO) of the hM4D (Gi) DREDD receptor and mCherry under the control of the oxytocin promoter (Fig. 5a). With this combination, we achieved DREADD(Gi)-mCherry expression exclusively in PVN OXT neurons projecting to the mPFC. We verified the regional specificity of virally mediated labeling of OXT neurons (Fig. 5b). We verified the regional and cell type specificity of virally mediated labeling of OXT neurons (Supplementary Fig. 10a). To control the efficacy of DREADD-mediated inhibition in PVN neurons retrogradely labeled from the mPFC, we performed ex vivo patch-clamp electrophysiology recordings on PVN slices. The results showed a significant reduction in the number of evoked spikes after CNO application in retrogradely labeled PVN neurons (Supplementary Fig. 10b, c). Selective inhibition of PNV-PFC oxytocinergic neuron projections had no effect on the duration in the central zone or open arm ratio without restraint stress. However, selective inhibition of OXT neurons projecting from the PVN to the mPFC was sufficient to reverse the PMS stress resilience phenotype (decreased duration in the central zone in the open field, Fig. 5c, d) and aggravate the anxiety level in standard-reared rats (decreased duration in the central zone in the open field test, Fig. 5g, h). The inhibition of PVN-mPFC OXT projection had no effects on locomotion ability (Fig. 5e, i). Altogether, these findings strengthen the conclusion that appropriate oxytocinergic signaling within the mPFC is critical to stress resilience, and PMS rats exhibited a resilient phenotype by increasing oxytocinergic signaling in the mPFC.

We investigated whether the oxytocin level could be correlated with key neurobiological features (i.e., anxiety, synaptic structures and transmissions and corticosterone response) in adult male rats. The oxytocin level in the mPFC inversely correlated with the corticosterone response in serum but showed a positive correlation with anxiety-like behavior (duration in central zones in the open field test and open arm ratio in the elevated plus maze test). Spine length and number showed a negative correlation with anxiety-like behavior and a positive correlation with corticosterone levels in serum. Synaptic transmission function was inversely correlated with spine length and number and negatively correlated with anxiety-like behavior (Supplementary Fig. 11). These findings are consistent with the overall conclusions from the results presented in rats, indicating that oxytocin expression is elevated in resilient PMS rats and is decreased in susceptible UMS rats. Together, these results identify that PMS exhibited stress resilience via an elevated oxytocin signaling pathway, while UMS exhibited stress susceptibility via a suppressed oxytocin signaling pathway.

DISCUSSION

Overall, our study provides direct evidence showing that predictable maternal separation leads to stress-reducing effects, while unpredictable maternal separation results in depression- and anxiety-like behavior, indicating that PMS promotes stress resilience and that UMS contributes to stress susceptibility.

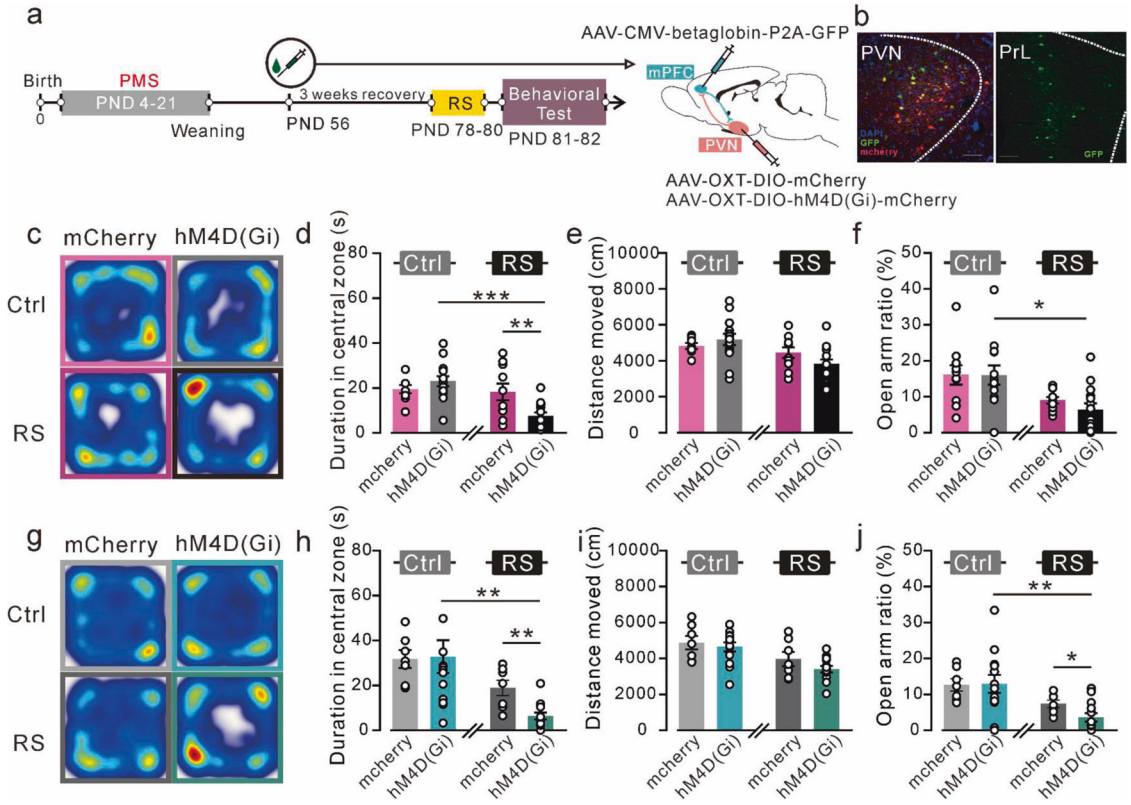

Fig. 5 PVN-mPFC OXT projections are necessary for anti-anxiety in PMS rats. a Timing of postnatal stress AAV manipulation, adult restraint stress and behavior testing and illustration of AAV injection into the mPFC and PVN. **b** Representative image of viral targeting of mPFC and PVN in adult male rat. Scale bar, 100 μm. **c** Heatmap of average rat exploration during open field test. **d** Duration in central zone in open field test (two-way ANOVA, interaction $F_{1,44} = 8.988$, $P = 0.004$, effect of restraint stress $F_{1,44} = 12.41$, $P = 0.001$, effect of AAV $F_{1,44} = 2.300$, $P = 0.136$). Restraint stress decreased duration in central zone significantly in PMS rats injected with hM4D (Gi) (Bonferroni post-test, $P < 0.001$), while RS has no effect on duration in PMS rats injected with mcherry (Bonferroni post-test, $P = 0.986$). After restraint stress, PMS rats injected with hM4D (Gi) spent less time in central zone compared to rats injected with mcherry (Bonferroni post-test, $P = 0.013$). **e** There was no difference in rats locomotor abilities (two-way ANOVA, interaction $F_{1,44} = 3.136$, $P = 0.084$; effect of RS $F_{1,44} = 0.975$, $P = 0.422$, effect of AAV $F_{1,44} = 0.222$, $P = 0.640$), indicating that locomotion ability of rats was not affected by PMS and restraint stress. **f** Open arm ratio in elevated plus maze (two-way ANOVA, interaction $F_{1,44} = 0.314$, $P = 0.578$, effect of restraint stress $F_{1,44} = 14.07$, $P = 0.001$, effect of AAV $F_{1,26} = 0.349$, $P = 0.558$). PMS rats injected with hM4D (Gi) spent less time in open arms after RS compared to rats before RS (Bonferroni post-test, $P = 0.012$). **g** Heatmap of average rat exploration during open field test. **h** Duration in central zone in open field test in standard-reared rats (two-way ANOVA, interaction $F_{1,36} = 1.544$, $P = 0.222$, effect of restraint stress $F_{1,36} = 12.84$, $P = 0.001$, effect of AAV $F_{1,36} = 6.081$, $P = 0.031$). Restraint stress decreased duration in central zone significantly in PMS rats injected with hM4D (Gi) (Bonferroni post-test, $P < 0.001$), while RS has no effect on duration in PMS rats injected with mcherry (Bonferroni post-test, $P = 0.986$). After restraint stress, PMS rats injected with hM4D (Gi) spent less time in central zone compared to rats injected with mcherry (Bonferroni post-test, $P = 0.004$). **i** There was no difference in rats locomotor abilities (two-way ANOVA, interaction $F_{1,36} = 0.329$, $P = 0.570$; effect of RS $F_{1,36} = 1.318$, $P = 0.138$, effect of AAV $F_{1,36} = 1.838$, $P = 0.184$). **j** Open arm ratio in elevated plus maze (two-way ANOVA, interaction $F_{1,36} = 0.967$, $P = 0.332$, effect of restraint stress $F_{1,36} = 12.88$, $P = 0.001$, effect of AAV $F_{1,36} = 0.801$, $P = 0.378$). Restraint stress decreased open arm ratio significantly in PMS rats injected with hM4D (Gi) (Bonferroni post-test, $P = 0.002$), while RS has no effect on duration in PMS rats injected with mcherry (Bonferroni post-test, $P = 0.383$). After restraint stress, PMS rats injected with hM4D (Gi) spent less time in open arms compared to rats injected with mcherry (Bonferroni post-test, $P = 0.046$). $^*P < 0.05$, $^{**}P < 0.01$, $^{***}P < 0.001$. Bar graphs show the mean ± s.e.m.

However, the undeniable fact is that previous studies support that maternal separation during the early life period contributes to the development of subsequent emotional instability [9, 18–21]. Many factors can lead to the different effects of maternal separation, including experimental design, strain differences, frequency, and predictability. Even maternal separation used in literature is similar to PMS, there are still other confounding factors leading to different results. Studies showed that 3 h of daily separation from birth to 14 days postnatal can result in depression-like behavior upon re-exposure to stress in adult rodents [22, 23]. While 3 h of maternal separation from PND 3-14 in Long-Evans rat pups did not appear to alter adult behaviors [24]. 4 h of maternal separation from PND 1–15 in Wistar rat had no effects on adult behaviors [25]. What's more, 3–4 h of separation from PND 1–13 can attenuate anxiety [26, 27], even 6 h of separation from PND 1–21 can lower emotional responses and decrease anxiety in adverse conditions in adults [28, 29]. But nearly none of the researchers have ever described the predictability or unpredictability of maternal separation. In our study, the duration and period of maternal separation and breeding environment are same in PMS and UMS rats. Unpredictable separation has more profound and persistent effects than predictable separation because it cannot be anticipated and compensated for [30]. Predictable separation is moderate early-life stress compared to unpredictable separation. Thus, divergent results of PMS and UMS confirmed the different effects of moderate and severe early-life stress on rat behaviors. Our findings support traditional theories about the stress-reducing role of predictability and are the first to examine in detail the effects of predictable and unpredictable maternal separation on adult rats. In addition, our results suggest that children with a prosperous early life are still susceptible to adult stress, while children who experience moderate predictable early-life stress,

such as setback education, could promote their resistance to adult stress, which provides parents with a sound theoretical basis for children's education.

However, the underlying mechanism by which unpredictable early-life stress leads to susceptibility and predictable stress results in resilience remains unclear. Our c-fos mapping data show that restraint stress activated more neuronal cells in the mPFC in PMS rats than in UMS rats. Dysfunction of the mPFC has been implicated in patients with anxiety, for which stress is a major risk factor [31]. Anxiety patients show reduced neuronal activity in the mPFC [32], and optogenetic stimulation corrects neural hypoactivity and rescues anxiety and anhedonia induced by social defeat [33]. Moreover, clinical studies indicate that brain stimulation within the prefrontal cortex can be effective for anxiety and severe treatment-resistant depression [34, 35]. Notably, stress results in structural and functional changes in the mPFC, including loss of dendritic spines and altered synaptic transmission. Consistently, we found that mPFC pyramidal neurons exhibited hypoactivity caused by reduced excitatory synaptic transmission and dendritic spine abnormalities in UMS rats but not in PMS rats. UMS may increase intracellular signaling in the mPFC, leading to morphological and physiological changes, which may be required for shaping adaptive behavioral responses in the face of adverse stress, thereby resulting in the development of susceptibility [36, 37]. To further reveal the effects of maternal separation on intracellular signaling, RNA-seq was applied to analyze the differentially expressed genes and signaling pathways.

Here, we elucidated the higher-order organization of the transcriptional response to separation stress across the mPFC and demonstrated oxytocin signaling as the main pathway to promote resilience in PMS rats. In humans, oxytocin has been proposed to play a role in the reduction of anxiety, and exogenous intranasally administered oxytocin has anxiolytic effects in anxiety disorder patients [38–40]. Central injection of oxytocin in rats and mice reduces anxiety [41, 42]. We showed that manipulations of OXT/OXTR significantly affected resilient/vulnerable behavior in PMS/UMS rats. Consistent with our results, activation of oxytocin receptor interneurons in the mouse mPFC is anxiolytic in males [43]. In our study, the manipulations of OXTR were altered the oxytocin concentration in mPFC. It is interpretable that OXTR knockdown/overexpression in mPFC neurons produces a reduction/increase in oxytocin levels. For a functional OXT-OXTR system, stimulus-dependent expression and release of OXT have to be balanced with a fine-tuned regulation of local OXTR expression [44]. Presynaptic oxytocin receptors were described in the 1980s by Audigier and Barberis [45]. The transfer of information via presynaptic receptors occurs in the direction from the synaptic cleft to the nerve terminals, which release the neurotransmitter [46]. In the early period, oxtr knockdown might lead to high oxytocin levels in the synaptic cleft. The high oxytocin level could affect the activation of oxtr on the presynaptic membrane, which might suppress oxytocin release to the synaptic cleft. Thus, we speculated that axon terminals possess presynaptic oxtrs that modulate oxytocin release through a negative-feedback mechanism. OXTR is the main target for endogenous and synthetic oxytocin. Oxytocin is supposed to be produced by PVN neurons, not only in the cell body but also in the axons. The regulation of oxytocin mRNA localization and local translation play vital roles in the maintenance of cellular structure and function [46]. Oxytocin mRNA localized in the mPFC can also be locally translated. To maintain the balance between oxytocin and OXTR, a reduction in OXTR in the mPFC might lead to a reduction in oxytocin levels. OXTR gene loss could lead to a reduction in oxytocin gene expression [47]. Further experiments are warranted to understand the mechanism. Although previous studies have revealed that oxytocin plays a pivotal role in anxiety behavior, they have never determined how to enhance the oxytocin level. In our research, the oxytocin level in the mPFC was upregulated in predictable separation rats, confirming that moderate early-life stress can raise oxytocin in the mPFC and then promote stress resilience in rats. However, how predictable maternal separation promotes oxytocin levels in the mPFC is not understood.

Notably, our manipulations of OXT/OXTR data support the existence of transcriptional analysis, as we repeatedly showed that manipulation of OXT/OXTR is sufficient to decrease resilience in rats with predictable separation by activating a network of vulnerable genes. Although our manipulation was limited to OXT/OXTR, some other genes associated with neuroinflammation were also enriched in PMS rats versus UMS rats. For example, interferon-stimulated gene-15 (Isg15), a ubiquitin-like protein (Ubl) that is expressed in response to type 1 interferon (IFN-α/β) signaling [48], was increased significantly in the mPFC of UMS rats compared to PMS rats and was upregulated following AAV-oxtr shRNA infection in the mPFC of PMS rats (data not shown). These observations show that manipulations of OXT/OXTR can cause downstream transcriptional effects in the mPFC. While neuroinflammation has been shown to play a role in anxiety and depression susceptibility [48], the role of oxytocin signaling and inflammation interaction in resilience has not yet been defined. These findings illustrate that the stress-reducing effects of predictable separation contribute to the oxytocin signaling pathway.

Overall, we have demonstrated that predictable early-life stress can promote stress resilience later in life, mediated by the oxytocin signaling pathway in the rat mPFC. Unpredictable maternal separation leads to depression-like/anxiety behavior, which becomes manifest after additional stress in adulthood. The steadily increasing burden of depression and anxiety highlights the need for improving their prevention and treatment. Understanding how moderate predictable early-life stress programs stress resilience provides insight into ways of preventing depression and anxiety disorders and reducing the deleterious effects of severe early-life stress.

DATA AVAILABILITY

The RNA-seq datasets analyzed during the current study are available in the figshare repository, [https://doi.org/10.6084/m9.figshare.15170274].

REFERENCES

1. Lupien SJ, McEwen BS, Gunnar MR, Heim C. Effects of stress throughout the lifespan on the brain, behaviour and cognition. Nat Rev Neurosci. 2009;10:434–45.
2. Nemeroff CB. Paradise lost: the neurobiological and clinical consequences of child abuse and neglect. Neuron. 2016;89:892–909.
3. Gunnar MR, Frenn K, Wewerka SS, Van Ryzin MJ. Moderate versus severe early life stress: associations with stress reactivity and regulation in 10-12-year-old children. Psychoneuroendocrinology. 2009;34:62–75.
4. Seery MD, Holman EA, Silver RC. Whatever does not kill us: cumulative lifetime adversity, vulnerability, and resilience. J Pers Soc Psychol. 2010;99:1025–41.
5. Schweizer S, Walsh ND, Stretton J, Dunn VJ, Goodyer IM, Dalgleish T. Enhanced emotion regulation capacity and its neural substrates in those exposed to moderate childhood adversity. Soc Cogn Affect Neurosci. 2016;11:272–81.
6. Harris MA, Brett CE, Starr JM, Deary IJ, McIntosh AM. Early-life predictors of resilience and related outcomes up to 66 years later in the 6-day sample of the 1947 Scottish mental survey. Soc Psychiatry Psychiatr Epidemiol. 2016;51:659–68.
7. Shapero BG, Hamilton JL, Stange JP, Liu RT, Abramson LY, Alloy LB. Moderate childhood stress buffers against depressive response to proximal stressors: a multi-wave prospective study of early adolescents. J Abnorm Child Psychol. 2015;43:1403–13.
8. Ladd CO, Owens MJ, Nemeroff CB. Persistent changes in corticotropin-releasing factor neuronal systems induced by maternal deprivation. Endocrinology. 1996;137:1212–8.
9. Pena CJ, Kronman HG, Walker DM, Cates HM, Bagot RC, Purushothaman I, et al. Early life stress confers lifelong stress susceptibility in mice via ventral tegmental area OTX2. Science. 2017;356:1185–8.
10. Vetulani J. Early maternal separation a rodent model of depression and a prevailing human condition. Pharmacol Rep. 2013;65:1451–61.

11. Biggio F, Pisu MG, Garau A, Boero G, Locci V, Mostallino MC, et al. Maternal separation attenuates the effect of adolescent social isolation on HPA axis responsiveness in adult rats. Eur Neuropsychopharmacol. 2014;24:1152–61.
12. Wetulani J. Early maternal separation a rodent model of depression and a prevailing human condition. Pharmacol Rep. 2013;65:1451–62.
13. Miller SM. Predictability and human stress: toward a clarification of evidence and theory. Adv Exp Soc Psychol. 1981;14:203–56.
14. Corbett BF, Luz S, Arner J, Pearson-Leary J, Sengupta A, Taylor D, et al. Sphingosine-1-phosphate receptor 3 in the medial prefrontal cortex promotes stress resilience by reducing inflammatory processes. Nat Commun. 2019;10:3146.
15. Plotsky PM, Meaney MJ. Early, postnatal experience alters hypothalamic corticotropin-releasing factor (CRF) mRNA, median eminence CRF content and stress-induced release in adult rats. Mol Brain Res. 1993;18:195–200.
16. Risher WC, Ustunkaya T, Singh Alvarado J, Eroglu C. Rapid Golgi analysis method for efficient and unbiased classification of dendritic spines. PLoS ONE. 2014;9:e107591.
17. Bourne J, Harris KM. Do thin spines learn to be mushroom spines that remember? Curr Opin Neurobiol. 2007;17:381–6.
18. Boku S, Toda H, Nakagawa S, Kato A, Inoue T, Koyama T, et al. Neonatal maternal separation alters the capacity of adult neural precursor cells to differentiate into neurons via methylation of retinoic acid receptor gene promoter. Biol Psychiatry. 2015;77:335–44.
19. Daniels WM, Pietersen CY, Carstens ME, Stein DJ. Maternal separation in rats leads to anxiety-like behavior and a blunted ACTH response and altered neurotransmitter levels in response to a subsequent stressor. Metab Brain Dis. 2004;19:3–14.
20. Authement ME, Kodangattil JN, Gouty S, Rusnak M, Symes AJ, Cox BM, et al. Histone deacetylase inhibition rescues maternal deprivation-induced GABAergic metaplasticity through restoration of AKAP signaling. Neuron. 2015;86:1240–52.
21. Liu C, Hao S, Zhu M, Wang Y, Zhang T, Yang Z. Maternal separation induces different autophagic responses in the hippocampus and prefrontal cortex of adult rats. Neuroscience. 2018;374:287–94.
22. Franklin TB, Linder N, Russig H, Thony B, Mansuy IM. Influence of early stress on social abilities and serotonergic functions across generations in mice. PLoS ONE. 2011;6:e21842.
23. Uchida S, Hara K, Kobayashi A, Funato H, Hobara T, Otsuki K, et al. Early life stress enhances behavioral vulnerability to stress through the activation of REST4-mediated gene transcription in the medial prefrontal cortex of rodents. J Neurosci. 2010;30:15007–18.
24. Shalev U, Kafkafi N. Repeated maternal separation does not alter sucrose-reinforced and open-field behaviors.pdf. Pharmacol Biochem Behav. 2002;73:115–22.
25. Marmendal M, Roman E, Eriksson CJ, Nylander I, Fahlke C. Maternal separation alters maternal care, but has minor effects on behavior and brain opioid peptides in adult offspring. Dev Psychobiol. 2004;45:140–52.
26. Macri S, Mason GJ, Wurbel H. Dissociation in the effects of neonatal maternal separations on maternal care and the offspring's HPA and fear responses in rats. Eur J Neurosci. 2004;20:1017–24.
27. de Jongh R, Geyer MA, Olivier B, Groenink L. The effects of sex and neonatal maternal separation on fear-potentiated and light-enhanced startle. Behav Brain Res. 2005;161:190–6.
28. Roman E, Gustafsson L, Berg M, Nylander I. Behavioral profiles and stress-induced corticosteroid secretion in male Wistar rats subjected to short and prolonged periods of maternal separation. Horm Behav. 2006;50:736–47.
29. Kaneko WM, Riley EP, Ehlers CL. Behavioral and electrophysiological effects of early repeated maternal separation. Depression. 1994;2:43–53.
30. Enthoven L, Oitzl MS, Koning N, van der Mark M, de Kloet ER. Hypothalamic-pituitary-adrenal axis activity of newborn mice rapidly desensitizes to repeated maternal absence but becomes highly responsive to novelty. Endocrinology. 2008;149:6366–77.
31. Simpson JR, Drevets WC, Snyder AZ, Gusnard DA, Raichle ME. Emotion-induced changes in human medial prefrontal cortex: II. During anticipatory anxiety. PNAS. 2001;98:688–93.
32. Zhao XH, Wang PJ, Li CB, Hu ZH, Xi Q, Wu WY, et al. Altered default mode network activity in patient with anxiety disorders: an fMRI study. Eur J Radio. 2007;63:373–8.
33. Covington HE III, Lobo MK, Maze I, Vialou V, Hyman JM, Zaman S, et al. Antidepressant effect of optogenetic stimulation of the medial prefrontal cortex. J Neurosci. 2010;30:16082–90.
34. Giacobbe P, Mayberg HS, Lozano AM. Treatment resistant depression as a failure of brain homeostatic mechanisms: implications for deep brain stimulation. Exp Neurol. 2009;219:44–52.
35. Bewernick BH, Hurlemann R, Matusch A, Kayser S, Grubert C, Hadrysiewicz B, et al. Nucleus accumbens deep brain stimulation decreases ratings of depression and anxiety in treatment-resistant depression. Biol Psychiatry. 2010;67:110–6.
36. Perova Z, Delevich K, Li B. Depression of excitatory synapses onto parvalbumin interneurons in the medial prefrontal cortex in susceptibility to stress. J Neurosci. 2015;35:3201–6.
37. Wang M, Perova Z, Arenkiel BR, Li B. Synaptic modifications in the medial prefrontal cortex in susceptibility and resilience to stress. J Neurosci. 2014;34:7485–92.
38. Missig G, Ayers LW, Schulkin J, Rosen JB. Oxytocin reduces background anxiety in a fear-potentiated startle paradigm. Neuropsychopharmacology. 2010;35:2607–16.
39. Windle RJ, Kershaw YM, Shanks N, Wood SA, Lightman SL, Ingram CD. Oxytocin attenuates stress-induced c-fos mRNA expression in specific forebrain regions associated with modulation of hypothalamo-pituitary-adrenal activity. J Neurosci. 2004;24:2974–82.
40. Kirsch P, Esslinger C, Chen Q, Mier D, Lis S, Siddhanti S, et al. Oxytocin modulates neural circuitry for social cognition and fear in humans. J Neurosci. 2005;25:11489–93.
41. Rotzinger S, Lovejoy DA, Tan LA. Behavioral effects of neuropeptides in rodent models of depression and anxiety. Peptides. 2010;31:736–56.
42. Sabihi S, Durosko NE, Dong SM, Leuner B. Oxytocin in the prelimbic medial prefrontal cortex reduces anxiety-like behavior in female and male rats. Psychoneuroendocrinology. 2014;45:31–42.
43. Li K, Nakajima M, Ibanez-Tallon I, Heintz N. A cortical circuit for sexually dimorphic oxytocin-dependent anxiety behaviors. Cell. 2016;167:60–72 e11.
44. Jurek B, Neumann ID. The oxytocin receptor: from intracellular signaling to behavior. Physiol Rev. 2018;98:1805–908.
45. Audigier S, Barberis C. Pharmacological characterization of two specific binding sites for neurohypophyseal hormones in hippocampal synaptic plasma membranes of the rat. EMBO J. 1985;4:1407–12.
46. Langer SZ. Presynaptic autoreceptors regulating transmitter release. Neurochem Int. 2008;52:26–30.
47. Vaidyanathan R, Hammock EAD. Oxytocin receptor gene loss influences expression of the oxytocin gene in C57BL/6J mice in a sex- and age-dependent manner. J Neuroendocrinol. 2020;32:e12821.
48. Blank T, Detje CN, Spiess A, Hagemeyer N, Brendecke SM, Wolfart J, et al. Brain endothelial- and epithelial-specific interferon receptor chain 1 drives virus-induced sickness behavior and cognitive impairment. Immunity. 2016;44:901–12.

ACKNOWLEDGEMENTS

This work was supported by grants from the National Natural Science Foundation of China (31900730), Shanghai Science and Technology Committee (20XD1423100, 19YF14420000), Shanghai Municipal Education Commission (2021-01-07-00-02-E0086), Shanghai Municipal Health Commission (2019ZB0201).

AUTHOR CONTRIBUTIONS

ZW and DDS conceived the study design. DDS performed all in vitro electrophysiology experiments, immunohistochemistry experiments and behavioral tests, with the help of YDZ and YYR; YDZ and SYP analyzed the behavioral test and electrophysiology experiments; DDS wrote the paper. ZW and TFY reviewed and edited the paper.

COMPETING INTERESTS

The authors declare no competing interests.

ADDITIONAL INFORMATION

Supplementary information The online version contains supplementary material available at https://doi.org/10.1038/s41380-021-01293-w.

Correspondence and requests for materials should be addressed to Zhen Wang.

Reprints and permission information is available at http://www.nature.com/reprints

Publisher's note Springer Nature remains neutral with regard to jurisdictional claims in published maps and institutional affiliations.